Amino Acids (2007) 32: 69–78
DOI 10.1007/s00726-006-0350-x
Printed in The Netherlands

Amino Acids

Molecular cloning of a cDNA encoding mouse D-aspartate oxidase and functional characterization of its recombinant proteins by site-directed mutagenesis

M. Katane, T. Furuchi, M. Sekine, and **H. Homma**

Laboratory of Biomolecular Science, School of Pharmaceutical Sciences, Kitasato University, Tokyo, Japan

Received January 24, 2006
Accepted March 15, 2006
Published online June 1, 2006;

Summary. The cDNA encoding D-aspartate oxidase (DASPO) was cloned from mouse kidney RNA by RT–PCR. Sequence analysis showed that it contained a 1023-bp open reading frame encoding a protein of 341 amino acid residues. The protein was expressed in *Escherichia coli* with or without an N-terminal His-tag and had functional DASPO activity that was highly specific for D-aspartate and *N*-methyl-D-aspartate. To investigate the roles of the Arg-216 and Arg-237 residues of the mouse DASPO (mDASPO), we generated clones with several single amino acid substitutions of these residues in an N-terminally His-tagged mDASPO. These substitutions significantly reduced the activity of the recombinant enzyme against acidic D-amino acids and did not confer any additional specificity to other amino acids. These results suggest that the Arg-216 and Arg-237 residues of mDASPO are catalytically important for full enzyme activity.

Keywords: D-aspartate oxidase – Flavoprotein – D-aspartate – Mouse – cDNA cloning – Site-directed mutagenesis

Abbreviations: D-Ala, D-alanine; D-Asn, D-asparagine; D-Asp, D-aspartate; BSA, bovine serum albumin; DAAO, D-amino acid oxidase; DASPO, D-aspartate oxidase; *E. coli*, *Escherichia coli*; FAD, flavin adenine dinucleotide; FMN, flavin mononucleotide; D-Glu, D-glutamate; His–mDASPO, N-terminally His-tagged mouse D-aspartate oxidase; IPTG, isopropyl-β-D-thiogalactopyranoside; mDASPO, mouse D-aspartate oxidase; D-Met, D-methionine; NMDA, *N*-methyl-D-aspartate; NMLA, *N*-methyl-L-aspartate; D-Pro, D-proline; SDS-PAGE, SDS-polyacrylamide gel electrophoresis

Introduction

All amino acids except glycine have an asymmetric α-carbon atom to which both amino and carboxyl groups attach, and they consequently have two kinds of stereoisomers, L- and D-forms. D-Amino acids have been regarded as unnatural isomers or laboratory artifacts, since various important functions of amino acids appear to be exerted only by L-amino acids. However, some D-amino acids were identified in the late 1960s as essential components of peptidoglycans in bacterial cell walls and of antibiotic peptides from bacteria (Osborn, 1969; Kreil, 1997). In addition, recent advances in analytical methods for separating chiral amino acids have revealed that several D-amino acids occur in various living organisms in their free form or in proteins. In mammals, free D-serine and D-aspartate (D-Asp) are present in a wide variety of tissues and cells, particularly in the central nervous and endocrine systems. Their physiological roles and metabolic pathways are now being investigated (Imai et al., 1996; Hashimoto and Oka, 1997; Fujii, 2002; Homma, 2002).

D-Asp oxidase (DASPO, EC 1.4.3.1) and D-amino acid oxidase (DAAO, EC 1.4.3.3) are known as flavin adenine dinucleotide (FAD)-containing flavoproteins that catalyze the oxidative deamination of D-amino acids by oxygen with the production of hydrogen peroxide, ammonia, and the corresponding 2-oxo acid. These two enzymes are similar in molecular weight, primary structure, and the type of catalytic reaction, but differ in substrate specificity. DAAO displays broad substrate specificity and oxidatively deaminates several neutral and basic D-amino acids, while DASPO is highly specific to acidic D-amino acids, such as D-Asp and D-glutamate (D-Glu), which are not substrates for DAAO. The physiological roles of these enzymes in vivo are diverse and not fully clarified. In microorganisms, these enzymes appear to be necessary for utilizing exogenous D-amino acids as growth substrates providing carbon and nitrogen. Recently, it was

also reported that DASPO plays an essential role in the assimilation and detoxification of D-Asp in yeast (Takahashi et al., 2005). The physiological roles of these enzymes in higher animals have been studied primarily in rodents. Yamada et al. (1988) first detected DASPO activity in mouse and rat tissues, and then demonstrated that the DASPO activity in mouse liver was increased by oral and intraperitoneal administrations of D-Asp, but not L-Asp (Yamada et al., 1989). In addition, oral administration of D-Asp and D-alanine (D-Ala) to mother rats during pregnancy and suckling increased the DASPO and DAAO activities, respectively, in the liver and kidneys of newborn rats (D'Aniello et al., 1993). Thus, current data suggests that the in vivo roles of DASPO and DAAO in higher animals are to detoxify and eliminate accumulated exogenous D-amino acids, in addition to regulating endogenous D-amino acid levels in various organs.

Recent advances in molecular biology techniques have enabled us to clone an interesting gene and prepare a large number of recombinant proteins overexpressed in heterologous organisms, such as *Escherichia coli* (*E. coli*) and yeast, and to dissect the biochemical properties of the proteins in vitro. This approach is an effective method for elucidating the physiological roles of the protein in detail. In fact, DAAO genes have been cloned from various organisms, including rodents such as mouse (Tada et al., 1990) and rat (Konno, 1998), and extensive mutagenesis experiments have been carried out to identify the amino acid residues responsible for enzymatic activity (Pilone, 2000; Tishkov and Khoronenkova, 2005). The three-dimensional structures of DAAOs from pig and from the yeast *Rhodotorula gracilis* have also been determined by X-ray crystallographic analyses (Mattevi et al., 1996; Mizutani et al., 1996; Umhau et al., 2000). Thus, a number of amino acid residues in the active site of DAAO have been identified and shown to play a significant role in substrate binding and in enzymatic activity. On the other hand, DASPO genes have been cloned only from bovine (Simonic et al., 1997), human (Setoyama and Miura, 1997), and the yeast *Cryptococcus humicola* (Takahashi et al., 2004). Gene cloning from rodents has not been reported, although they have been widely used to study the physiological roles of DASPO, as described above. Mutagenesis experiments and crystallographic analysis of DASPO are yet to be reported. Hence, there are few findings as to the active site of DASPO.

In this study, we first cloned a cDNA encoding DASPO from mouse kidney and expressed the recombinant mouse DASPO (mDASPO) in *E. coli*. To identify the amino acid residues responsible for the enzymatic activity of mDASPO, we prepared several mutants of mDASPO in which a single amino acid residue predicted to be located in active site by modeling of the three-dimensional structure of mDASPO was substituted by other amino acid residues. In addition, the biochemical properties of these mutants were investigated and compared with those of recombinant wild-type mDASPO. This is the first report of cDNA cloning of rodent DASPO and of site-directed mutagenesis of DASPO.

Materials and methods

Animals and chemicals

Adult male 129/Sv mice were obtained from the Laboratory of Public Health and Molecular Toxicology (School of Pharmaceutical Sciences, Kitasato University, Japan).

D- and L-amino acids, bovine serum albumin (BSA), and DAAO from porcine kidney (1.2 units/mg solid, lyophilized powder) were purchased from Sigma Chemical Co. (St. Louis, MO, USA). FAD, flavin mononucleotide (FMN), isopropyl-β-D-thiogalactopyranoside (IPTG), benzoic acid, malonic acid, and *meso*-tartaric acid were purchased from Wako Pure Chemical Industries (Osaka, Japan). Other chemicals were of the highest available grade and purchased from commercial sources.

Isolation of an mDASPO cDNA clone

Total RNA was extracted from the kidney of an adult male 129/Sv mouse with ISOGEN reagent (Nippon Gene, Tokyo, Japan), according to the manufacturer's instructions. For first strand cDNA synthesis, the RNA samples (3 μg) were reverse-transcribed for 60 min at 42 °C in a 20 μl reaction volume with 200 units of SuperScript II Reverse Transcriptase and 0.5 μg of oligo $(dT)_{12–18}$ primer (Invitrogen, Carlsbad, CA, USA). The mDASPO cDNA sequence was identified in the nucleotide sequence database at NCBI (National Center for Biotechnology Information) using the sequence of the human DASPO-1 cDNA (GenBank accession number: D89858) as the query in a BLAST search (URL: http://www.ncbi.nlm.nih.gov/blast/). The mDASPO cDNA was amplified by PCR using the first strand cDNA as a template and the following primers, 5′-TTTCA GAGACAGGCCATGGAC-3′ and 5′-AGGATCATGCCAGCTCTAGG-3′. The PCR product was cloned into pT7Blue-2 (Novagen, Madison, WI, USA) and sequenced (pT7Blue-2-mDASPO).

Construction of recombinant protein expression plasmids

For construction of N-terminally His-tagged mDASPO (His–mDASPO) expression plasmid, the 1.1-kbp *Nco*I–*Hin*dIII fragment containing the entire mDASPO-coding sequence of pT7Blue-2-mDASPO was subcloned into pRSET-B (Invitrogen) to generate the His–mDASPO expression plasmid (pRSET-His–mDASPO). This plasmid was then digested with *Nde*I and *Kpn*I to remove the N-terminal His-tag and treated with Klenow fragment polymerase, followed by self-ligation, resulting in the native mDASPO expression plasmid (pRSET-mDASPO).

From the pRSET-His–mDASPO plasmid, seven plasmids were produced by site-directed mutagenesis (QuikChange II Site-Directed Mutagenesis Kit, Stratagene, La Jolla, CA, USA), each containing a single amino acid substitution: Arg-216-to-Met (R216M), Arg-216-to-Ala (R216A), Arg-216-to-Glu (R216E), Arg-216-to-Leu (R216L), Arg-237-to-Tyr (R237Y), Arg-237-to-Ala (R237A), or Arg-237-to-Glu (R237E).

The mutagenic oligonucleotides, with the mutated codons underlined, were as follows:

for R216M, 5′-CTGGGTGAAGCATTTCATCATGGATGGGGGCGGGCTG-3′ and
5′-CAGCCCGCCCCCATCCATGATGAAATGCTTCACCCAG-3′;
for R216A, 5′-GGTGAAGCATTTCATCGCAGATGGGGGCGGG-3′ and
5′-CCCGCCCCCATCTGCGATGAAATGCTTCACC-3′;
for R216E, 5′-GGGTGAAGCATTTCATCGAGGATGGGGGCGGGC-3′ and
5′-GCCCGCCCCCATCCTCGATGAAATGCTTCACCC-3′;
for R216L, 5′-GGGTGAAGCATTTCATCTTAGATGGGGGCGGGC-3′ and
5′-GCCCGCCCCCATCTAAGATGAAATGCTTCACCC-3′;
for R237Y, 5′-GTAACCCTGGGAGGAACTTACCAGAAAGGAGACTGGAATCG-3′ and
5′-CGATTCCAGTCTCCTTTCTGGTAAGTTCCTCCCAGGGTTAC-3′;
for R237A, 5′-ACCCTGGGAGGAACTGCACAGAAAGGAGACTGG-3′ and
5′-CCAGTCTCCTTTCTGTGCAGTTCCTCCCAGGGT-3′;
for R237E, 5′-GTAACCCTGGGAGGAACTGAGCAGAAAGGAGACTGGAATCG-3′ and
5′-CGATTCCAGTCTCCTTTCTGCTCAGTTCCTCCCAGGGTTAC-3′.

The introduction of the desired mutations was confirmed by sequencing.

Expression of recombinant proteins

E. coli strain BL21(DE3)pLysS cells transformed with the expression plasmids were grown in Luria-Bertani medium containing ampicillin (100 μg/ml) at 30 °C with shaking. When the absorbance at 620 nm reached 0.5, IPTG was added to a final concentration of 0.01 mM, and the cells were grown at 30 °C for an additional 20 h. The cells were pelleted by centrifugation at 10,000 *g* for 10 min at 4 °C. The pellets were resuspended in lysis buffer consisting of BugBuster Protein Extraction Reagent (Novagen) and protease inhibitors (Roche Applied Science, Mannheim, Germany) using 5 ml lysis buffer per gram of wet cell paste, and the cell suspension was incubated for 20 min at room temperature with gently shaking. The resultant lysates were centrifuged at 12,000 *g* for 20 min at 4 °C to pellet insoluble cell debris. The supernatant (crude extract) was filtered through a 0.45 μm membrane filter (Asahi Techno Glass Co., Tokyo, Japan), and stored frozen at −80 °C until use. For the preparation of whole cell lysates, a fraction of the cultured cells was withdrawn during the cultivation and pelleted by centrifugation at 10,000 *g* for 10 min at 4 °C. The pellets were then resuspended in phosphate-buffered saline, mixed with an equal volume of 4% SDS solution, and boiled immediately.

For mutagenesis experiments, *E. coli* strain JM 109 transformant cells were grown in Luria-Bertani medium containing ampicillin (100 μg/ml) at 22 °C with shaking. When the absorbance at 620 nm reached 0.8, the cells were pelleted by centrifugation at 10,000 *g* for 10 min at 4 °C. Crude extracts were prepared as described above.

Detection of recombinant proteins

The protein levels in whole cell lysates and crude extracts were determined by the method of Bradford (1976) using BSA as a standard. Proteins present in whole cell lysates were separated on a 12% SDS–polyacrylamide gel (SDS–PAGE) and stained with Coomassie Brilliant Blue R-250. Broad range molecular weight standards (Bio-Rad, Hercules, CA, USA) were used as the molecular weight marker proteins. Crude extracts were subjected to 12% SDS–PAGE and Western blotting using anti-His-tag (His-probe, Santa Cruz Biotechnology, Santa Cruz, CA, USA) (1:1000) as a primary antibody and horseradish peroxidase-conjugated anti-rabbit IgG (Jackson ImmunoResearch Laboratories, West Grove, PA, USA) (1:5000) as a secondary reagent. The protein bands were visualized with an enhanced chemiluminescence reagent (Amersham Biosciences, Piscataway, NJ, USA) and exposure to X-ray film.

Enzymatic activity assays

Oxidase activity was determined by colorimetric measurement of 2-oxo acid produced from the corresponding amino acid. Crude extracts, prepared as described above (20 and 40 μg from *E. coli* strain BL21(DE3)-pLysS and JM 109 transformant cells, respectively), were mixed with a reaction mixture consisting of 40 mM sodium pyrophosphate buffer (pH 8.3), 67 μM FAD, and 20 mM amino acid in a final volume of 150 μl, and incubated at 37 °C for 30 min. Subsequently 10 μl of 100% trichloroacetic acid was added, and proteins were pelleted by centrifugation at 20,000 *g* for 10 min at 4 °C. The supernatant (150 μl) was mixed with 100 μl of 2,4-dinitrophenylhydrazine in 2 M HCl, and incubated at 37 °C for 15 min, then 750 μl of 3.75 M NaOH was added, and the solution was cleared by centrifugation at 20,000 *g* for 10 min at 4 °C. The absorbance of the supernatant at 445 nm was measured against the blank prepared from a reaction mixture without amino acid. One unit of enzyme activity was defined as the production of 1 μmol of the corresponding 2-oxo acid per min, under the above assay conditions. For inhibition of the activity, an inhibitor, benzoate, malonate, or *meso*-tartrate, was added to the reaction mixture. In some cases, DAAO from porcine kidney (2 μg) was used as control instead of crude extract.

In mutagenesis experiments, enzyme activities obtained were corrected as follows. In order to determine the amounts of the recombinant proteins in crude extracts, the intensities of the protein bands visualized by Western blotting (see Fig. 5) were estimated by densitometric scanning using Image SXM (version 1.74) software. The enzyme activity values were divided by these estimated protein amounts, and the resultant values were used to calculate the percent activity relative to that obtained with crude extract prepared from cells transformed with wild-type His–mDASPO plasmid.

Results

Isolation and sequence analysis of mDASPO cDNA

We searched the nucleotide sequence database at NCBI with the human DASPO-1 cDNA sequence (Setoyama and Miura, 1997) to identify a mouse cDNA clone (GenBank accession number: BC027312) that had a high degree of identity to the human DASPO-1 cDNA. Based on the sequence of the cDNA clone, a set of primers was designed. Using these primers and total RNA extracted from mouse kidney, a 1423-bp DNA fragment was amplified by RT-PCR. Sequence analysis revealed that the amplified DNA consisted of a 15-bp 5′-untranslated region, a 1023-bp open reading frame, and a 385-bp 3′-untranslated region (Fig. 1). It also showed that five nucleotides in the open reading frame differed from the sequence deposited in the database. Namely, the G at nt201, A at nt296, T at nt490, A at nt834, and C at nt942 were T, G, A, G, and T, respectively, in the database sequence for mDASPO (Fig. 1).

The open reading frame encodes a protein of 341 amino acids (Fig. 1) with a calculated molecular mass of 37,617 Da. The amino acid sequence contained the

```
-15                                                          tttcagagacaggcc

  1  ATGGACACAGTGTGTATTGCGGTCGTTGGAGCTGGCGTGATAGGGCTGTCTACTGCAGCA
  1  M  D  T  V  C  I  A  V  V  G  A  G  V  I  G  L  S  T  A  A

 61  TGCATTTCCCAACTGGTTCCCGGATGCACCGTCACTGTCATCTCAGACAGGTTCACTCCT
 21  C  I  S  Q  L  V  P  G  C  T  V  T  V  I  S  D  R  F  T  P

121  GATACCACCAGTAATGTAGCGGCTGGGATGCTTATTCCTCACACGTATGCAGATACCCCG
 41  D  T  T  S  N  V  A  A  G  M  L  I  P  H  T  Y  A  D  T  P

181  GTGCCCACGCAGAAGCGATGGTTTAGAGAGACCTTCGAGCATCTTTCTGAAATCGCCAAG
 61  V  P  T  Q  K  R  W  F  R  E  T  F  E  H  L  S  E  I  A  K

241  TCTGCAGAGGCTGCAGATGCGGGTGTTCACCTGGTATCTGGTTGGCAGATATTCCACAGC
 81  S  A  E  A  A  D  A  G  V  H  L  V  S  G  W  Q  I  F  H  S

301  GTCCCCGCTGAAGAAGTGCCTTTCTGGGCTGATGTGGTGCTGGGATTTCGAAAGATGACA
101  V  P  A  E  E  V  P  F  W  A  D  V  V  L  G  F  R  K  M  T

361  GAGGCTGAGCTGAAGCGGTTCCCTCAGTATGTGTTTGGCCAGGCTTTTACAACCCTGAAG
121  E  A  E  L  K  R  F  P  Q  Y  V  F  G  Q  A  F  T  T  L  K

421  TGCGAGACTTCTGCCTACCTCCCGTGGCTGGAGAGAAGGATAAAGGGGAGTGGAGGTCTG
141  C  E  T  S  A  Y  L  P  W  L  E  R  R  I  K  G  S  G  G  L

481  CTACTCACCTGGAGAATAGAAGACCTGTGGGAGCTGCAGCCATCTTTTGATATCGTGGTC
161  L  L  T  W  R  I  E  D  L  W  E  L  Q  P  S  F  D  I  V  V

541  AATTGCTCAGGCCTGGGAAGCCGGCGACTTGTAGGTGACCCCATGATTTCCCCGGTAAGG
181  N  C  S  G  L  G  S  R  R  L  V  G  D  P  M  I  S  P  V  R

601  GGCCAGGTGCTCCAGGCACGGGCCCCCTGGGTGAAGCATTTCATCCGAGATGGGGGCGGG
201  G  Q  V  L  Q  A  R  A  P  W  V  K  H  F  I  R  D  G  G  G

661  CTGACTTATGTTTACCCTGGTATGTCCTATGTAACCCTGGGAGGAACTAGACAGAAAGGA
221  L  T  Y  V  Y  P  G  M  S  Y  V  T  L  G  G  T  R  Q  K  G

721  GACTGGAATCGATCCCCAGATGCAGAACTTAGCAGAGAGATTTTTTCTCGATGCTGCACT
241  D  W  N  R  S  P  D  A  E  L  S  R  E  I  F  S  R  C  C  T

781  CTCGAGCCTTCCCTCCACAGAGCCTACGACATAAAAGAGAAAGTGGGGCTGAGACCCAGC
261  L  E  P  S  L  H  R  A  Y  D  I  K  E  K  V  G  L  R  P  S

841  AGGCCAGGTGTGCGGCTGCAGAAGGAGATCCTAGTCCGGGGACAACAGACGCTGCCTGTG
281  R  P  G  V  R  L  Q  K  E  I  L  V  R  G  Q  Q  T  L  P  V

901  GTCCACAACTACGGCCACGGGAGTGGGGGCATCTCTGTGCACTGGGGCTCTGCTCTGGAA
301  V  H  N  Y  G  H  G  S  G  G  I  S  V  H  W  G  S  A  L  E

961  GCCACCAGGCTGGTGATGGAGTGTATCCATACCCTCAGGACCCCTGCTTCCTTGTCGAAG
321  A  T  R  L  V  M  E  C  I  H  T  L  R  T  P  A  S  L  S  K

1021 CTGtagctgacaccaagtaacagcagctaatccaggtgatatgggtcaaagcacaattta
 341 L  *

1081 aggtccgtaactgggtctcgtaactttcatactgcttgaacgttgagtctgaccttcttt
1141 gtttttacgcaatgagtatcagtagacttagaaagcttgtcagtaatgacacagaacaca
1201 aagctcggtttttgtcaaaatatgtgctatttaaaaatacttgttctatggggtagattt
1261 ggggaggatcgaatgctaacttatatgaatgatgtaagcgatagggagttcatattttg
1321 gctcagaagcacataagcacataagagaagattaatgtgtgagaaatatacttggctccc
1381 tgtcagccctagagctgtgcatgatcct
```

Fig. 1. Nucleotide sequence of mDASPO cDNA and its deduced amino acid sequence. The amino acid sequence is shown in the single letter code below each nucleotide codon. Nucleotide and amino acid numbers are indicated at the left. An asterisk below the nucleotide sequence indicates a stop codon. The FAD-binding motif (GXGXXG) is underlined. The type 1 peroxisomal targeting signal consisting of the C-terminal three amino acids is double-underlined. Each nucleotide distinct from that in the mouse cDNA clone in the NCBI database is indicated by a dot

FAD-binding consensus sequence, GXGXXG at residues 10–15, and a C-terminal consensus sequence -(S/A/C)-(K/R/H)-L that is a type 1 peroxisomal targeting signal (Gould et al., 1989). In comparison with other reported amino acid sequences of DASPOs and DAAOs, the encoded protein showed a high degree of identity to human DASPO-1 (80.4%) and bovine DASPO (75.4%), while it showed only a moderate degree of identity to the yeast *Cryptococcus humicola* DASPO (28.0%) and DAAOs from various organisms including mouse (24.9–41.5%). Likewise, phylogenetic analysis revealed that the encoded protein formed a cluster with human DASPO-1 and bovine DASPO (data not shown), suggesting that they were evolutionarily derived from a single gene.

Expression of the recombinant proteins in E. coli and their enzymatic activities against D-Asp

To confirm that the cloned cDNA really encodes the functional DASPO, the mDASPO and His–mDASPO expression plasmids under the control of the T7 promoter were constructed. His–mDASPO is a protein of 382 amino acid residues with a calculated molecular mass of 42,074 Da. *E. coli* strain BL21(DE3)pLysS cells that overexpress T7 polymerase after IPTG addition were transformed with each expression construct, and total cell lysates were prepared from the transformant cells. Intense protein bands were detected in lysates from cells exposed to IPTG for 20 h, whereas these bands were not detected in cells lysed before IPTG exposure (Fig. 2). The apparent molecular masses of these recombinant proteins were in good agreement with those calculated from their deduced amino acid sequences. No band was detected in lysates from cells transformed with the parental plasmid regardless of the incubation time after IPTG addition (Fig. 2).

We examined the enzymatic activity of the recombinant proteins against D- and L-Asp. Crude extracts prepared from the transformed cells 20 h after IPTG addition were used as enzyme. The enzymatic activity against D-Asp was reproducibly detected in crude extract from cells transformed with the mDASPO plasmid, whereas the activity against L-Asp was negligible. The mean ± standard deviation from four independent preparations was 113.3 ± 34.8 and 0.7 ± 0.3 mU/mg protein for D- and L-Asp, respectively. Like the mDASPO extract, the His-mDASPO extract showed activity against D-Asp, but not L-Asp. The mean ± standard deviation from four independent preparations was 102.9 ± 29.5 and 0.5 ± 0.3 mU/mg protein for D- and L-Asp, respectively. Crude extract from cells transformed with the parental plasmid had no activity against either D- or L-Asp (data not shown). Collectively, the protein encoded by the cloned cDNA possesses the enzymatic activity to deaminate D-Asp, and our data indicate that the His-tag sequence at the N-terminus did not affect the activity of the recombinant mDASPO.

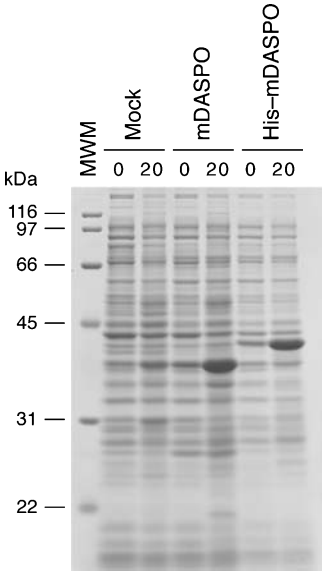

Fig. 2. Expression of recombinant mDASPO and His–mDASPO in *E. coli*. Proteins (20 µg) in whole cell lysates were separated on a 12% SDS–polyacrylamide gel and stained with Coomassie Brilliant Blue R-250. mDASPO, His–mDASPO, and Mock indicate lysates from *E. coli* strain BL21(DE3)pLysS cells transformed with the mDASPO plasmid, the His–mDASPO plasmid, and the parental plasmid, pRSET-B, respectively. The incubation time (h) after IPTG addition is indicated above each lane. *MWM* Molecular weight marker proteins

Enzymatic and functional characterization of the recombinant proteins

To examine whether the recombinant proteins have the same properties as other DASPOs, we examined the FAD dependency of the enzymatic activity of the recombinant mDASPO and His–mDASPO. Lack of FAD in the reaction mixture markedly reduced the activity against D-Asp in mDASPO and His–mDASPO extracts (Table 1), suggesting that a large fraction of the recombinant proteins in crude extracts exists as apoenzyme that does not bind to endogenous FAD from *E. coli*. Addition of FMN, the precursor of FAD, had no effect on the activity. These results indicate that the catalytic mechanisms of the recombinant proteins were FAD-dependent, consistent with previous reports of the coenzyme requirement of DASPOs (Yamada et al., 1988; Kera et al., 1992, 1996).

Table 1. FAD dependency of the enzymatic reaction catalyzed by the recombinant mDASPO and His–mDASPO

Condition[a]		Relative activity (%)[b]	
FAD	FMN	mDASPO	His–mDASPO
+	–	100 ± 2.3	100 ± 2.5
–	–	5.8 ± 1.8	4.0 ± 0.4
–	+	10.1 ± 0.2	4.6 ± 1.2

[a] For samples without FAD and FMN, a reaction mixture without D-Asp and FAD was used as the blank

[b] Percent activity relative to that obtained in the presence of D-Asp and FAD is shown. The absorbance at 445 nm with crude extracts from the transformed cells expressing recombinant mDASPO and His–mDASPO were 1.231 and 0.575, respectively. Each value shown is the mean ± standard deviation of triplicate assays

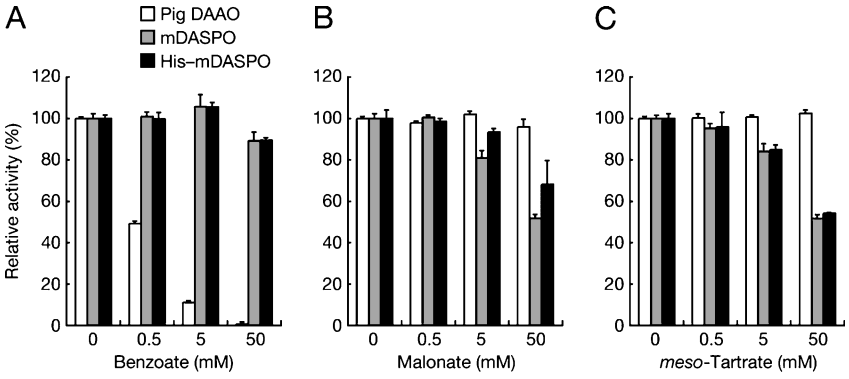

Fig. 3. Effects of inhibitors on recombinant mDASPO and His–mDASPO. Enzyme activity was assayed using pig DAAO (white bars), mDASPO extract (grey bars), and His–mDASPO extract (black bars) in the presence of the indicated concentrations of benzoate (**A**), malonate (**B**), and *meso*-tartrate (**C**). Substrates used were D-Ala for pig DAAO and D-Asp for mDASPO and His–mDASPO extracts. Percent activity relative to that obtained in the absence of the inhibitors is shown. The pig DAAO absorbance at 445 nm was 0.703, 0.736, and 0.666 for **A**, **B**, and **C**, respectively; the mDASPO extract absorbance at 445 nm was 1.281, 1.240, and 1.173 for **A**, **B**, and **C**, respectively; the His–mDASPO extract absorbance at 445 nm was 0.570, 0.511, and 0.580 for **A**, **B**, and **C**, respectively. Each value shown is the mean ± standard deviation of a triplicate assay

We then examined the effects of benzoate, malonate, and *meso*-tartrate on the enzymatic activity. As shown in Fig. 3A, benzoate, a known selective inhibitor of DAAO, had no effect on the activity of mDASPO and His–mDASPO against D-Asp, even at a concentration of 50 mM. In contrast, the oxidase activity of pig DAAO against D-Ala was almost completely inhibited. However, malonate, a known selective inhibitor of DASPO, reduced the activity of mDASPO and His–mDASPO against D-Asp to 52 and 68% of the controls, respectively, at a concentration of 50 mM (Fig. 3B). Similarly, increasing concentrations of *meso*-tartrate, another selective inhibitor of DASPO, reduced the activity of mDASPO and His–mDASPO against D-Asp to 52 and 54% of the controls, respectively (Fig. 3C). Malonate and *meso*-tartrate had no effect on the oxidase activity of pig DAAO against D-Ala. These selective inhibitions and the magnitude of the inhibitions are consistent with previous characterizations of DASPOs and DAAOs (Yamada et al., 1988; Kera et al., 1992, 1996; Sarower et al., 2003).

Since human DASPO-1 and bovine DASPO, which show a high degree of identity to mDASPO at the amino acid level, were reported to efficiently deaminate *N*-methyl-D-Asp (NMDA) in addition to D-Asp (Setoyama and Miura, 1997; Negri et al., 1999), the substrate specificity of the recombinant mDASPO and His–mDASPO was examined. Activity against NMDA was detected in the mDASPO extract at a similar level to that against D-Asp (Table 2). In contrast, *N*-methyl-L-Asp (NMLA), which is an enantiomer of NMDA, was not a good substrate. The activities against D-Glu and all neutral D-amino acids examined were very low or undetectable. His–mDASPO showed a substrate specificity similar to mDASPO (Table 2). Consequently, mDASPO and His–mDASPO showed the enzymatic hallmarks of DASPO, confirming that the cloned cDNA really encodes a functional DASPO which is highly specific to D-Asp and NMDA.

Table 2. Substrate specificity of the recombinant mDASPO and His–mDASPO

Substrate[a]	Relative activity (%)[b]	
	mDASPO	His–mDASPO
D-Asp	100 ± 24	100 ± 24
NMDA	83 ± 14	97 ± 22
D-Glu	14 ± 3.5	6.3 ± 0.9
D-Asn	15 ± 12	6.3 ± 1.1
D-Met	1.8 ± 0.8	4.4 ± 3.1
D-Ala	0.2 ± 0.1	1.0 ± 0.2
D-Pro	<0.1	<0.1
L-Asp	<0.1	0.8 ± 0.7
NMLA	4.0 ± 0.9	2.6 ± 0.2

[a] *D-Asn* D-asparagine; *D-Met* D-methionine; *D-Pro* D-proline

[b] Percent activity relative to that obtained with D-Asp as a substrate is shown. The absorbance at 445 nm with crude extracts from the transformed cells expressing recombinant mDASPO and His–mDASPO were 1.144 and 0.575, respectively. Each value shown is the mean ± standard deviation from three independent assays

Mutagenesis experiments on amino acid residues located in the active site of mDASPO

In order to identify the amino acid residues located in the active site and responsible for the enzymatic activity of mDASPO, the following experiments were conducted.

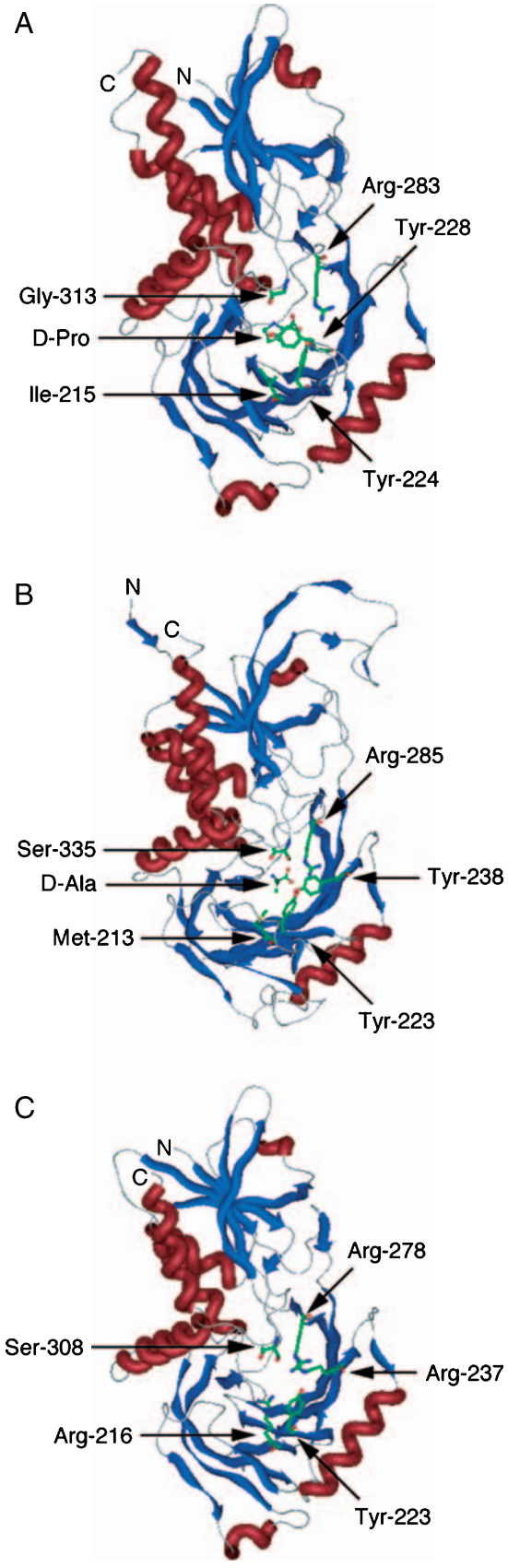

Since the three-dimensional structures of DAAOs from pig and the yeast *Rhodotorula gracilis* have already been reported in complex with their substrates (Mizutani et al., 1999; Umhau et al., 2000), we searched the amino acid residues that were adjacent to the substrates in these DAAOs using the Swiss-Pdb Viewer (version 3.7) software. Eight and seven amino acid residues were found to be located at a distance $\leq$4.5 Å from the substrates in pig and *Rhodotorula gracilis* DAAOs, respectively. Of these amino acid residues, Ile-215, Tyr-224, Tyr-228, Arg-283, and Gly-313 residues in pig DAAO and Met-213, Tyr-223, Tyr-238, Arg-285, and Ser-335 residues in *Rhodotorula gracilis* DAAO were located at structurally equivalent positions (Fig. 4A, B). Alignment of the amino acid sequence of mDASPO with those of the pig and *Rhodotorula gracilis* DAAOs suggested that the corresponding residues of mDASPO were Arg-216, Tyr-223, Arg-237, Arg-278, and Ser-308 (data not shown). This was supported by a model of the three-dimensional structure of mDASPO (Fig. 4C), which was generated with the SWISS-MODEL server (Peitsch, 1995; Guex and Peitsch, 1997; Schwede et al., 2003) using the deduced amino acid sequence of mDASPO (Fig. 1). In this model, the side chains of Arg-216, Tyr-223, Arg-237, Arg-278, and Ser-308 were oriented toward the predicted binding pocket of the active site, suggesting that these amino acid residues are catalytically important.

In the current study, we focused on the Arg-216 and Arg-237 residues of mDASPO, and constructed several derivatives of the His–mDASPO gene in which the codon for Arg-216 was mutated to that for Glu (His–mDASPO-R216E), Met (His–mDASPO-R216M), Leu (His–mDASPO-R216L), or Ala (His–mDASPO-R216A), or the codon for Arg-237 was mutated to that for Glu (His–mDASPO-R237E), Tyr (His–mDASPO-R237Y), or Ala (His–mDASPO-R237A). R216E and R237E are charge reversal mutations. The amino acid residues corresponding to Arg-216 and Arg-237 of mDASPO were predicted to be Met-213 and Tyr-238,

Fig. 4. Mapping of key catalytic residues in the predicted three-dimensional structure of mDASPO. Experimentally determined structures of pig DAAO in complex with D-Pro (Mizutani et al., 1999) and yeast *Rhodotorula gracilis* DAAO in complex with D-Ala (Umhau et al., 2000) are shown in **A** and **B**, respectively. Substrates are presented using ball and stick structures. For clarity, FAD molecules have been omitted. A proposed structural model of mDASPO is shown in **C**. Side chains of amino acid residues presumed to be catalytically important are presented as cylinders. The letters *N* and *C* indicate the N- and C-terminus of the protein, respectively

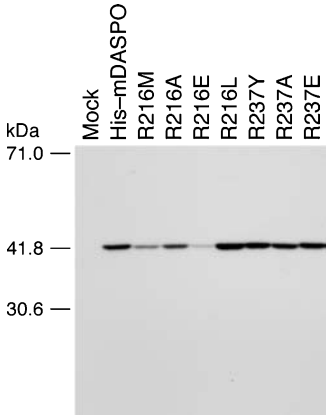

Fig. 5. Expression of mutant proteins of His–mDASPO in *E. coli*. Cellular expression of the His–mDASPO mutants was examined by Western blotting of the crude extracts (20 µg) using an anti-His-tag antibody. His–mDASPO, R216M, R216A, R216E, R216L, R237Y, R237A, R237E, and Mock indicate crude extracts from *E. coli* JM 109 cells transformed with the wild-type His–mDASPO, His–mDASPO-R216M, His–mDASPO-R216A, His–mDASPO-R216E, His–mDASPO-R216L, His–mDASPO-R237Y, His–mDASPO-R237A, His–mDASPO-R237E, and the parental pRSET-B plasmids, respectively

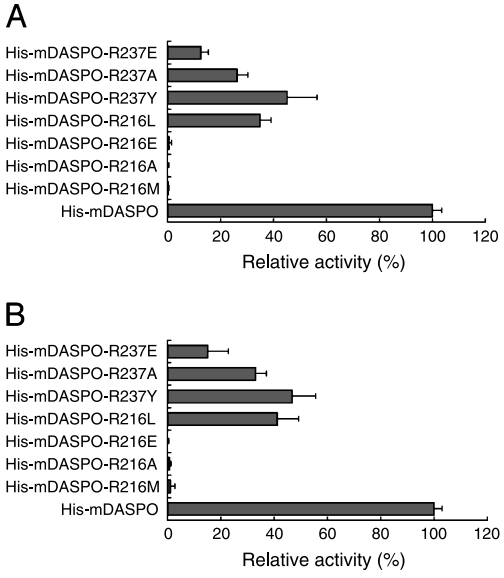

Fig. 6. Enzymatic activity of His–mDASPO mutants against D-Asp (**A**) and NMDA (**B**). Enzymatic activity was assayed using crude extracts from *E. coli* JM 109 cells expressing the indicated proteins. Percent activity relative to the wild-type His–mDASPO extract is shown. The wild-type His–mDASPO absorbance at 445 nm was 0.389 and 0.342 for **A** and **B**, respectively. Relative amounts of the recombinant proteins in crude extracts were determined by densitometric scanning of the bands detected by Western blot (Fig. 5) using Image SXM (version 1.74) software, and the enzymatic activity was corrected based on the relative amount of the expressed proteins. Each value shown is the mean ± standard deviation from three independent assays

respectively, of *Rhodotorula gracilis* DAAO (Fig. 4B, C), and alignment of the amino acid sequence of mDASPO with that of mouse DAAO suggested that the corresponding residues of mouse DAAO were Leu-213 and Tyr-226 (data not shown). Based on these findings, the R216M, R216L, and R237Y mutations were introduced into His–mDASPO in order to render its active site more similar to the active site of *Rhodotorula gracilis* and/or mouse DAAOs. R216A and R237A mutations were also introduced, since the non-polar Ala residue which does not generate steric hindrance is frequently used as a control substitution. *E. coli* strain JM 109 cells were transformed with the expression constructs encoding these mDASPO mutants, and the recombinant proteins were detected in crude extracts (Fig. 5).

Subsequently, we examined the enzymatic activity of these mutant proteins against amino acid substrates listed in Table 2. As shown in Fig. 6A, moderate activity against D-Asp was detected in crude extracts from the R216L, R237E, R237Y, and R237A mutants, but the activities were significantly lower than the wild-type His–mDASPO. Likewise, these extracts showed moderate activity against NMDA (Fig. 6B). More importantly, the R216E, R216M, and R216A mutants lost virtually all activity against both D-Asp and NMDA. The activities against substrates other than D-Asp and NMDA were very low or undetectable in all of the mutants (data not shown). Taken together, these results indicate that the Arg-216 and Arg-237 residues of mDASPO are most likely to function as key catalytic residues for the full enzymatic activity of mDASPO.

Discussion

Five nucleotides in the open reading frame of mDASPO cDNA cloned from the 129/Sv mouse strain differed from the sequence previously deposited in the NCBI database (Fig. 1). Trp-67, His-99, and Trp-164 in the amino acid sequence of mDASPO reported in this study are Cys, Arg, and Arg residues, respectively, in the NCBI sequence. These differences are likely to be strain specific, since the nucleotide sequence in the database is derived from the C57BL/6 mouse strain. In the deduced amino acid sequence of mDASPO (Fig. 1), the C-terminal three amino acids were SKL, which corresponds to a consensus sequence of the type 1 peroxisomal targeting signal (Gould et al., 1989). mDASPO is thus predicted to be localized to peroxisomes, similar to human DASPO-1 (Amery et al., 1998) and bovine DASPO (Zaar, 1996). Since enzymatic reactions catalyzed by DASPO and DAAO produce hydrogen peroxide that is toxic to cells,

localization of these enzymes in the peroxisome which includes hydrogen peroxide-degrading catalase seems to be beneficial to the survival of cells metabolizing D-amino acids.

The present study demonstrates that a functional recombinant mDASPO can be expressed in *E. coli* regardless of the presence of a N-terminal His-tag sequence. It should be noted, however, that a large fraction of the recombinant mDASPO and His–mDASPO expressed in *E. coli* accumulated in an insoluble form when examined by SDS–PAGE (data not shown). Modifications in the concentration of IPTG, culture temperature, and incubation time after IPTG addition did not improve the recovery of these recombinant proteins in the soluble fraction. A weak enzyme activity against D-Glu (Table 2) may be one of the factors that limit recovery in the soluble fraction. D-Glu in *E. coli* is an essential component of peptidoglycans (Mengin-Lecreulx, 1982), and therefore the recombinant enzymes may be sequestered as inactive insoluble forms for this reason. Furthermore, the oxidative deamination of D-Glu produces hydrogen peroxide which is highly toxic to *E. coli*. It may be necessary to prepare the recombinant proteins in eukaryotic cells, such as yeast and insect cells for improved recovery.

To our knowledge, this is the first report of a mutagenesis study on DASPO. Since the three-dimensional structure of DASPO has not been determined, we proposed a structural model of mDASPO using the SWISS-MODEL server (Peitsch, 1995; Guex and Peitsch, 1997; Schwede et al., 2003). Based on comparison of this model with the experimentally determined structures of DAAOs from the pig and the yeast *Rhodotorula gracilis* (Mizutani et al., 1996; Umhau et al., 2000), we focused on the Arg-216 and Arg-237 residues of mDASPO. Using His–mDASPO mutants in the present study, our findings indicate that these residues of mDASPO play an important role in the enzymatic reaction, conceivably by being involved in the active center. Notably, the R216M, R216L and R237Y mutant enzymes do not oxidize neutral D-amino acids. This contrasted with a previous report that an M213R mutant of the yeast *Rhodotorula gracilis* DAAO displayed specificity toward acidic D-amino acids in addition to its normal specificity for neutral D-amino acids (Sacchi et al., 2002). Since Met-213 in *Rhodotorula gracilis* DAAO corresponds to Arg-216 in mDASPO, the R216M mutant enzyme was expected to have a broad specificity to neutral D-amino acids in addition to its normal specificity for acidic D-amino acids. Similarly, Leu-213 in mouse DAAO corresponds to Arg-216 in mDASPO, so the R216L mutant enzyme was expected to show a broad specificity to neutral D-amino acids provided that the Arg-216 residue of mDASPO functions as a key residue in binding of the substrate. In this study, catalytically important residues of mDASPO were predicted to be Arg-216, Tyr-223, Arg-237, Arg-278, and Ser-308. Of these amino acid residues, Tyr-223, Arg-278, and Ser-308 are conserved in DAAOs of the pig and/or yeast *Rhodotorula gracilis*, while Arg-216 and Arg-237 are not (Fig. 4). Therefore, we considered the possibility that Arg-237 of mDASPO plays an essential role in selecting the substrate, and this residue, which corresponds to the Tyr-228 and Tyr-238 residues of the pig and *Rhodotorula gracilis* DAAOs, respectively (Fig. 4), was substituted by a Tyr residue with the expectation that the substrate specificity of the R237Y mutant enzyme would be more similar to that of these DAAOs. Further studies are necessary to identify the amino acid residue(s) involved in the strict specificity for acidic D-amino acids.

Finally, the recombinant DASPO will be a valuable tool for the rapid and convenient detection of acidic D-amino acids in biological and food samples. The recombinant His–mDASPO can be purified in a single chromatographic step using a chelating column. However its recovery in the soluble fraction was low, as described above. Further studies will be necessary to optimize conditions for the expression of this recombinant protein for its eventual use in practical applications.

Acknowledgements

The authors would like to thank Azusa Nakajima, Yuri Iijima, Maki Yoshimoto, Shiho Saitoh, Mari Watanabe, and Mika Watanabe for technical assistance.

References

Amery L, Brees C, Baes M, Setoyama C, Miura R, Mannaerts GP, Van Veldhoven PP (1998) C-terminal tripeptide Ser-Asn-Leu (SNL) of human D-aspartate oxidase is a functional peroxisome-targeting signal. Biochem J 336: 367–371

Bradford MM (1976) A rapid and sensitive method for the quantitation of microgram quantities of protein utilizing the principle of protein-dye binding. Anal Biochem 72: 248–254

D'Aniello A, D'Onofrio G, Pischetola M, D'Aniello G, Vetere A, Petrucelli L, Fisher GH (1993) Biological role of D-amino acid oxidase and D-aspartate oxidase. Effects of D-amino acids. J Biol Chem 268: 26941–26949

Fujii N (2002) D-Amino acids in living higher organisms. Orig Life Evol Biosphere 32: 103–127

Gould SJ, Keller GA, Hosken N, Wilkinson J, Subramani S (1989) A conserved tripeptide sorts proteins to peroxisomes. J Cell Biol 108: 1657–1664

Guex N, Peitsch MC (1997) SWISS-MODEL and the Swiss-PdbViewer: an environment for comparative protein modeling. Electrophoresis 18: 2714–2723

Hashimoto A, Oka T (1997) Free D-aspartate and D-serine in the mammalian brain and periphery. Prog Neurobiol 52: 325–353

Homma H (2002) D-Aspartate in the mammalian body. Viva Origino 30: 204–215 (available online at http://www.origin-life.gr.jp/3004/3004204/3004204.pdf)

Imai K, Fukushima T, Santa T, Homma H, Hamase K, Sakai K, Kato M (1996) Analytical chemistry and biochemistry of D-amino acids. Biomed Chromatogr 10: 303–312

Kera Y, Aoyama H, Watanabe N, Yamada R (1996) Distribution of D-aspartate oxidase and free D-glutamate and D-aspartate in chicken and pigeon tissues. Comp Biochem Physiol B Biochem Mol Biol 115: 121–126

Kera Y, Nagasaki H, Iwashima A, Yamada R (1992) Presence of D-aspartate oxidase and free D-aspartate in amphibian (*Xenopus laevis*, *Cynops pyrrhogaster*) tissues. Comp Biochem Physiol B 103: 345–348

Konno R (1998) Rat D-amino-acid oxidase cDNA: rat D-amino-acid oxidase as an intermediate form between mouse and other mammalian D-amino-acid oxidases. Biochim Biophys Acta 1395: 165–170

Kreil G (1997) D-Amino acids in animal peptides. Annu Rev Biochem 66: 337–345

Mattevi A, Vanoni MA, Todone F, Rizzi M, Teplyakov A, Coda A, Bolognesi M, Curti B (1996) Crystal structure of D-amino acid oxidase: a case of active site mirror-image convergent evolution with flavocytochrome b_2. Proc Natl Acad Sci USA 93: 7496–7501

Mengin-Lecreulx D (1982) Cytoplasmic steps of peptidoglycan synthesis in *Escherichia coli*. J Bacteriol 151: 1109–1117

Mizutani H, Miyahara I, Hirotsu K, Nishina Y, Shiga K, Setoyama C, Miura R (1996) Three-dimensional structure of porcine kidney D-amino acid oxidase at 3.0 Å resolution. J Biochem (Tokyo) 120: 14–17

Negri A, Tedeschi G, Ceciliani F, Ronchi S (1999) Purification of beef kidney D-aspartate oxidase overexpressed in *Escherichia coli* and characterization of its redox potentials and oxidative activity towards agonists and antagonists of excitatory amino acid receptors. Biochim Biophys Acta 1431: 212–222

Osborn MJ (1969) Structure and biosynthesis of the bacterial cell wall. Annu Rev Biochem 38: 501–538

Peitsch MC (1995) Protein modeling by E-mail. Bio/Technology 13: 658–660

Pilone MS (2000) D-Amino acid oxidase: new findings. Cell Mol Life Sci 57: 1732–1747

Sacchi S, Lorenzi S, Molla G, Pilone MS, Rossetti C, Pollegioni L (2002) Engineering the substrate specificity of D-amino-acid oxidase. J Biol Chem 277: 27510–27516

Sarower MG, Matsui T, Abe H (2003) Distribution and characteristics of D-amino acid and D-aspartate oxidases in fish tissues. J Exp Zoolog A Comp Exp Biol 295: 151–159

Schwede T, Kopp J, Guex N, Peitsch MC (2003) SWISS-MODEL: An automated protein homology-modeling server. Nucleic Acids Res 31: 3381–3385

Setoyama C, Miura R (1997) Structural and functional characterization of the human brain D-aspartate oxidase. J Biochem (Tokyo) 121: 798–803

Simonic T, Duga S, Negri A, Tedeschi G, Malcovati M, Tenchini ML, Ronchi S (1997) cDNA cloning and expression of the flavoprotein D-aspartate oxidase from bovine kidney cortex. Biochem J 322: 729–735

Tada M, Fukui K, Momoi K, Miyake Y (1990) Cloning and expression of a cDNA encoding mouse kidney D-amino acid oxidase. Gene 90: 293–297

Takahashi S, Kakuichi T, Fujii K, Kera Y, Yamada R (2005) Physiological role of D-aspartate oxidase in the assimilation and detoxification of D-aspartate in the yeast *Cryptococcus humicola*. Yeast 22: 1203–1212

Takahashi S, Takahashi T, Kera Y, Matsunaga R, Shibuya H, Yamada R (2004) Cloning and expression in *Escherichia coli* of the D-aspartate oxidase gene from the yeast *Cryptococcus humicola* and characterization of the recombinant enzyme. J Biochem 135: 533–540

Tishkov VI, Khoronenkova SV (2005) D-amino Acid oxidase: structure, catalytic mechanism, and practical application. Biochemistry (Mosc) 70: 40–54

Umhau S, Pollegioni L, Molla G, Diederichs K, Welte W, Pilone MS, Ghisla S (2000) The x-ray structure of D-amino acid oxidase at very high resolution identifies the chemical mechanism of flavin-dependent substrate dehydrogenation. Proc Natl Acad Sci USA 97: 12463–12468

Yamada R, Nagasaki H, Nagata Y, Wakabayashi Y, Iwashima A (1989) Administration of D-aspartate increases D-aspartate oxidase activity in mouse liver. Biochim Biophys Acta 990: 325–328

Yamada R, Nagasaki H, Wakabayashi Y, Iwashima A (1988) Presence of D-aspartate oxidase in rat liver and mouse tissues. Biochim Biophys Acta 965: 202–205

Zaar K (1996) Light and electron microscopic localization of D-aspartate oxidase in peroxisomes of bovine kidney and liver: an immunocytochemical study. J Histochem Cytochem 44: 1013–1019

Authors' address: Hiroshi Homma, Laboratory of Biomolecular Science, School of Pharmaceutical Sciences, Kitasato University, 5-9-1 Shirokane, Minato-ku, Tokyo 108-8641, Japan,
Fax: +81-3-5791-6381, E-mail: hommah@pharm.kitasato-u.ac.jp